Available online at www.sciencedirect.com
SCIENCE DIRECT
European Journal of Pharmaceutics and Biopharmaceutics 59 (2005) 351–358
European Journal of Pharmaceutics and Biopharmaceutics
www.elsevier.com/locate/ejpb

Research paper

Use of roughness maps in visualisation of surfaces

Paulus Seitavuopio[a,*], Jukka Rantanen[b], Jouko Yliruusi[a,b]

[a]Faculty of Pharmacy, Pharmaceutical Technology Division, University of Helsinki, Helsinki, Finland
[b]Viikki Drug Discovery Technology Center, University of Helsinki, Helsinki, Finland

Received 17 March 2004; accepted in revised form 13 September 2004
Available online 10 November 2004

Abstract

In this study we will present a new method to describe surface roughness. This method builds a roughness map of the studied area. The roughness map can give information of localised roughness. The test surfaces used in the evaluation of the method were tablets, which were made of lactose monohydrate, theophylline anhydrate, sodium chloride and potassium chloride. The roughness determinations were made by a laser profilometer. The new matrix method gives detailed roughness maps, which are able to show local variations in surface roughness values and provide an illustrative picture of the heterogeneity of surface roughness of various materials.

Keywords: Laser profilometer; Scanning electron microscopy (SEM); Tablet; Surface; Roughness; Roughness map

1. Introduction

Surface roughness is a critical parameter in various fields of material sciences. In painting, for example, the surface should contain some degree of roughness in order to provide enough adhesion between the paint and the subject surface. Also different kinds of papers have very different degrees of surface roughness, since there are different types of paper qualities e.g. for laser printing, ink-jet printing and newspaper. With pharmaceutics, surface roughness influences particle flow properties, wettability, surface friability, and the quality of final tablet coating. In the granulation and coating processes the surface roughness presumably has a remarkable effect on the adhesion of the polymer solution on the surface.

One well-established method for surface roughness measurement is non-contact laser profilometry or optical profilometry which has previously been used in pharmacy [1–5]. Laser profilometry has also been used in many different fields of material research like paper coating, dental materials and surgical prosthesis [6–8]. Laser profilometry is accurate, quantitative, flexible method and it can be used to study areas with diameters up to several centimetres. Problems with the laser profilometer can arise with materials, which have poor reflection properties.

Various roughness calculation methods have previously been used in the literature, but these methods often give only one value for the roughness of the surface, and they fail to visualize or give regional information of the roughness on the surface [1,2]. Fractal dimension has been also used to characterise surface roughness in different size scales [9–12]. On the other hand, it has been shown that the measured roughness is dependent on the size of the measurement area and the resolution [13].

The purpose of this study was to describe a new method, which can give information of localised roughness across a wider area and build up easily readable roughness maps of the surfaces. The test surfaces used in the evaluation of the new 'matrix method' were tablets made of lactose monohydrate, theophylline anhydrate, sodium chloride and potassium chloride.

* Corresponding author. Faculty of Pharmacy, Pharmaceutical Technology Division, University of Helsinki, P.O. Box 56, Helsinki 00014, Finland. Tel.: +358 9 19159661; fax: +358 9 19159144.
E-mail address: paulus.seitavuopio@helsinki.fi (P. Seitavuopio).
URL: http://www.pharmtech.helsinki.fi/.

0939-6411/$ - see front matter © 2004 Elsevier B.V. All rights reserved.
doi:10.1016/j.ejpb.2004.08.009

2. Materials and methods

2.1. Materials

The materials in this study were M325 lactose monohydrate (DMV International, Netherlands) and Ph. Eur. grade of theophylline anhydrate (BASF, Ludvigshafen, Germany); for reference purposes, materials used were analytical-grade of sodium chloride (NaCl) (Riedel-de Haën, Germany) and potassium chloride (KCl) (Riedel-de Haën, Germany). The particle size of the powders was determined with a Leica MZ-6 optical microscope (Leica DMLB, Leica Microskopie and Systeme GmbH, Germany) which was equipped with Leica QWin image-analysis software (Leica QWin V2.6, Leica DMLB, Leica Microskopie and Systeme GmbH, Germany). At least 800 particles were used in each particle size determination by measuring the horizontal and the vertical dimensions of which the averages were calculated.

2.2. Tablet compression

Tablets were compressed with a 13 mm evacuable IR tablet die (Specac Ltd, UK) and a hydraulic press (Pye Unicam, UK). The compression forces were 30 and 80 kN and the compression time was 2 min. Corresponding compression pressures were 225 and 600 MPa. The tablet die was evacuated by a vacuum pump during the compression in order to get strong and non-breakable tablets. Tablet weight varied from 300 to 450 mg. Prepared tablets were attached to metal sample plates with double-sided tape in order to assist in the handling and identification of the correct tablet surface.

2.3. Surface characterisation

2.3.1. Scanning electron microscopy

An SEM (Zeiss DSM 962, Germany) was used in order to obtain a large and accurate view of the tablet surfaces. The SEM pictures were also used as a reference for the laser profilometer measurements. The magnifications used were 200 lactose monohydrate and 500 for theophylline anhydrate, respectively.

2.3.2. Laser profilometry

Tablet surface roughness was measured with a laser profilometer (UBM Microfocus Measurement System, UBM Messtechnik GMbH, Ettlingen, Germany), which was also used to get 3D images from tablet surfaces. Tablet surfaces were studied using an image size of 2×2 mm and the resolution of 1000 points/mm. The roughness values R_a and R_{rms} were determined from one 2×2 mm area of each sample. After data collection the image data was levelled to remove slope caused by tilting of the tablet surface and tilting caused by the sample plate and double-sided tape using a data-analysis programme (Ubsoft version 2.8 DOS, UBM Messtechnik GMbH, Ettlingen, Germany). Laser profilometer images, showing actual measurement height data (2000×2000 data points per image), were further analysed by Mathematica 4.0 programme (Wolfram Research, USA).

2.3.3. Roughness parameters and roughness maps

Two basic roughness parameters R_a and R_{rms} were used in this study.

The average roughness (R_a) parameter was calculated from the height data according to Eq. (1)

$$R_a = \sum_{n=1}^{N} \frac{|Z_n - \bar{Z}|}{N}, \quad (1)$$

where Z_n was the individual height value of one measurement point and $\bar{Z}$ the mean value of all the height data points. N was the number of measurement points. The root mean square roughness (R_{rms}) was calculated from the standard deviation of the height data (Eq. (2)).

$$R_{rms} = \frac{\sqrt{\sum_{n=1}^{N}(Z_n - Z^2)}}{N-1} \quad (2)$$

The roughness parameters R_a and R_{rms} were calculated in two different ways: first by the standard method using the analysis program submitted with the equipment (Ubsoft version 2.8 DOS, UBM Messtechnik GMbH, Ettlingen, Germany) and then by our new matrix method, which gives

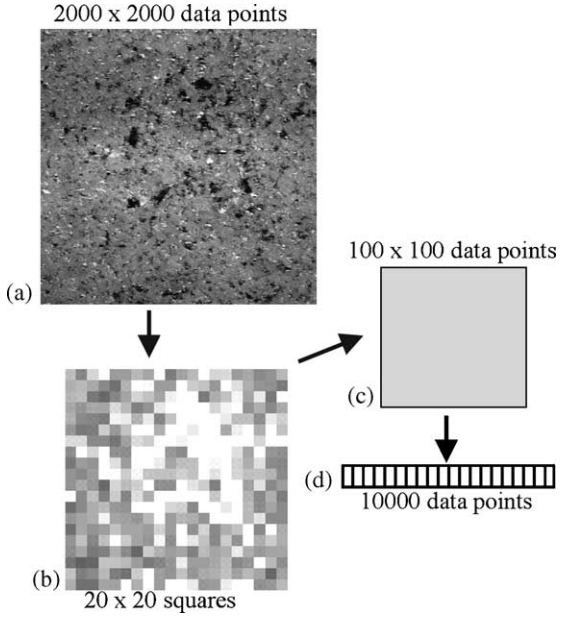

Fig. 1. Scheme of the matrix calculation method. (a) The original laser profilometer image (2×2 mm) showing the actual height differences, (b) the roughness map (2×2 mm) calculated from the same image, (c) one of the 400 squares (100×100 μm) and (d) the 10,000 measurement points in the square were organised into a row of numbers from which the roughness parameters R_a and R_{rms} were calculated.

detailed localized roughness information of the surface. The standard method gave single roughness value for both the R_a and R_{rms} parameters describing the whole measured 2×2 mm area.

In the new matrix method the 2×2 mm areas (corresponding 4 million data points) were divided in to 400 small squares (squared matrixes) and the R_a and R_{rms} roughness parameters of those squared matrixes were calculated using Mathematica 4.0 programme (Wolfram Research, USA) (Fig. 1). The size of the squares was chosen to be 10,000 points in order to achieve adequate statistical significance for the local surface roughness estimates. Similar division of the measured area into smaller sections has been described earlier in literature by Yoshinobu et al. [11], but they used the sectioning for measurement of scale independent roughness from atomic force microscope images. In this paper the R_a roughness values of the small squares were drawn to roughness maps which illustrate the variation of the roughness on the different areas of sample surface. The roughness values in the roughness maps were scaled between 0 and 1 to enhance differences in the maps. The roughness maps were used to condense the large amount of information in the original laser profilometer images. By this way the roughness maps help to visualise the differences in local roughness.

3. Results and discussion

3.1. Scanning electron microscopy

SEM images suggested that with lactose monohydrate and theophylline anhydrate, higher compression pressure produced surfaces where holes or gaps between particles were smaller because the higher compression pressure packed the particles denser to each other (Fig. 2a–d). The smaller holes between particles yield smaller roughness. Original particle borders can be seen better in the case of lactose monohydrate tablets, but original 'crystals' were also visible from the theophylline anhydrate tablets. The size of the powder particles are given in Table 1. In the lactose monohydrate tablets with lower compression pressure there were a number of small particles visible on the surface which could not be seen on the tablets compressed with the higher compression pressure. On the 80 kN lactose monohydrate and theophylline anhydrate tablets the holes between larger particles seemed to be filled up with smaller particles. This suggested that fragmentation is the main compaction phenomenon which created smoother surfaces. Lactose monohydrate has been described so as to compress mainly with fragmentation, which can lead to the formation of small particles filling the holes between larger particles [14–16]. On the other hand,

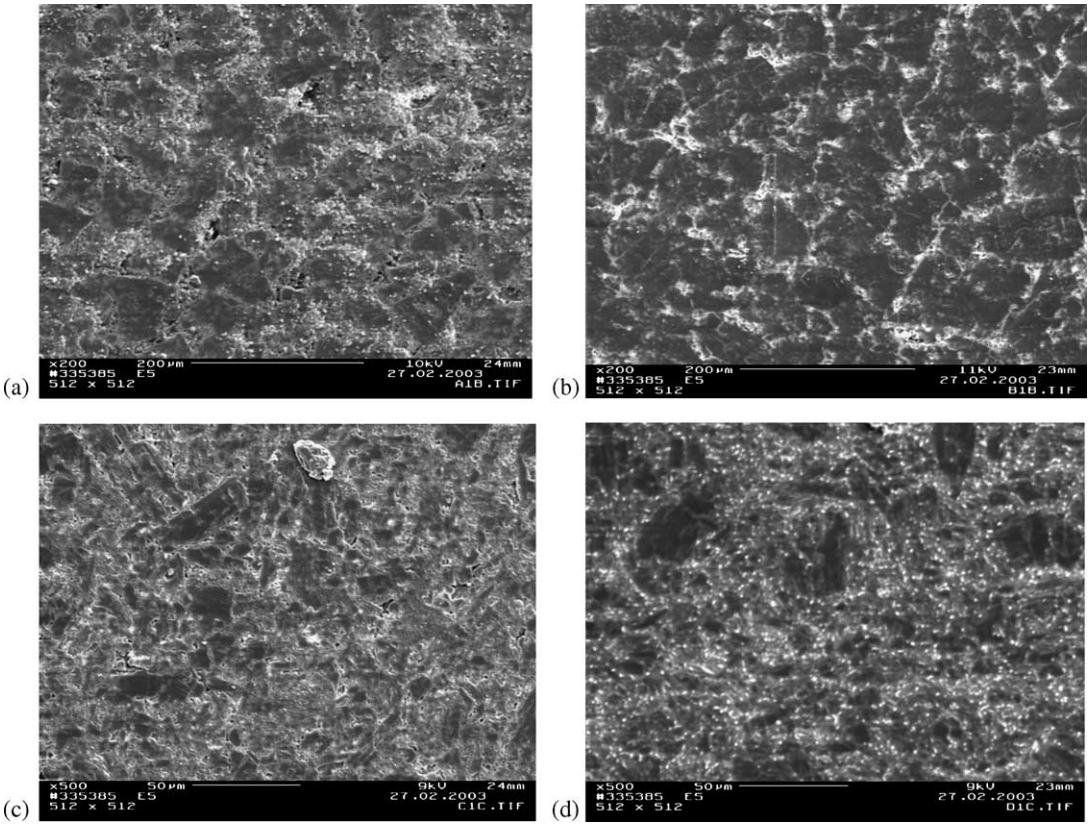

Fig. 2. SEM micrographs of the tablets. (a) 30 kN lactose monohydrate tablet, (b) 80 kN lactose monohydrate tablet, (c) 30 kN theophylline anhydrate tablet and (d) 80 kN theophylline anhydrate tablet.

Table 1
Particle size of the original powders measured by image analysis ($n=800$)

	Mean ± SD (μm) ($n=800$)	Max (μm)	Min (μm)
Lactose monohydrate	32 ± 27	190	2
Theophylline anhydrate	43 ± 26	190	2
KCl	190 ± 92	680	22
NaCl	210 ± 130	660	14

theophylline anhydrate has been described to compress with plastic flow at compression pressures below 150 MPa [17]. It might be possible that with the higher compression pressures (225 and 600 MPa) used in this study, theophylline anhydrate particles fragment which might explain the smaller particles seen in the 80 kN theophylline anhydrate tablets.

3.2. Laser profilometry and roughness

The laser profilometer images also showed that higher compression pressure produces smoother surfaces because the particles were packed denser (Figs. 3a–d and 4a–f). The original powder particles were nearly visible in the laser profilometer images (Figs. 3a and b and 4a and b). Especially with lactose monohydrate, both size and amount of holes or gaps between the larger particles were smaller with the higher compression pressure (Fig. 3a and b). Similar behaviour has been observed earlier with sodium chloride and potassium chloride [5]. In the Fig. 3a the area with the largest holes was marked with a line and the same area was marked also on the corresponding roughness map (Fig. 5a). The roughness differences were also clear in the line profiles of the lactose monohydrate tablets (Fig. 3c and d). The effect of lower and higher compression pressures on the surface structure in the case of theophylline anhydrate was not as clear as with lactose monohydrate, but some difference in the roughness of the tablets can be seen in the line profiles (Fig. 4c–f). The particle size of lactose monohydrate was larger and therefore the original particles were more easily detectable in the tablet surfaces than with the theophylline anhydrate tablets (Figs. 3a and b and 4a and b). It also pointed out that usually the reflectance images did not give any additional features from tablet surfaces. However, in the case of the theophylline the largest crystals were better visible in the reflectance mode (data not shown).

The roughness values of the standard method calculated by the laser profilometer measurement and data-analysis programme (Ubsoft version 2.8 DOS, UBM Messtechnik

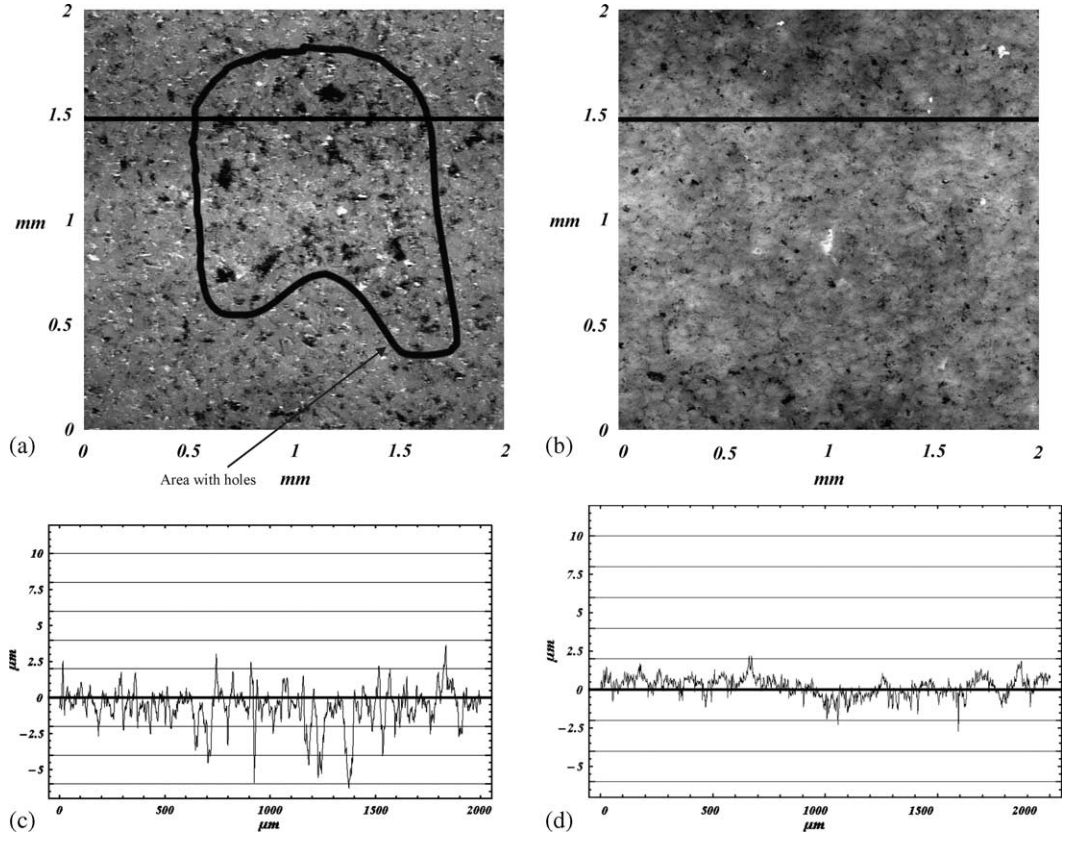

Fig. 3. Laser profilometer images of the lactose monohydrate tablets. (a) 30 kN lactose monohydrate tablet, (b) 80 kN lactose monohydrate tablet, (c) profile line from (a), and (d) profile line from (b).

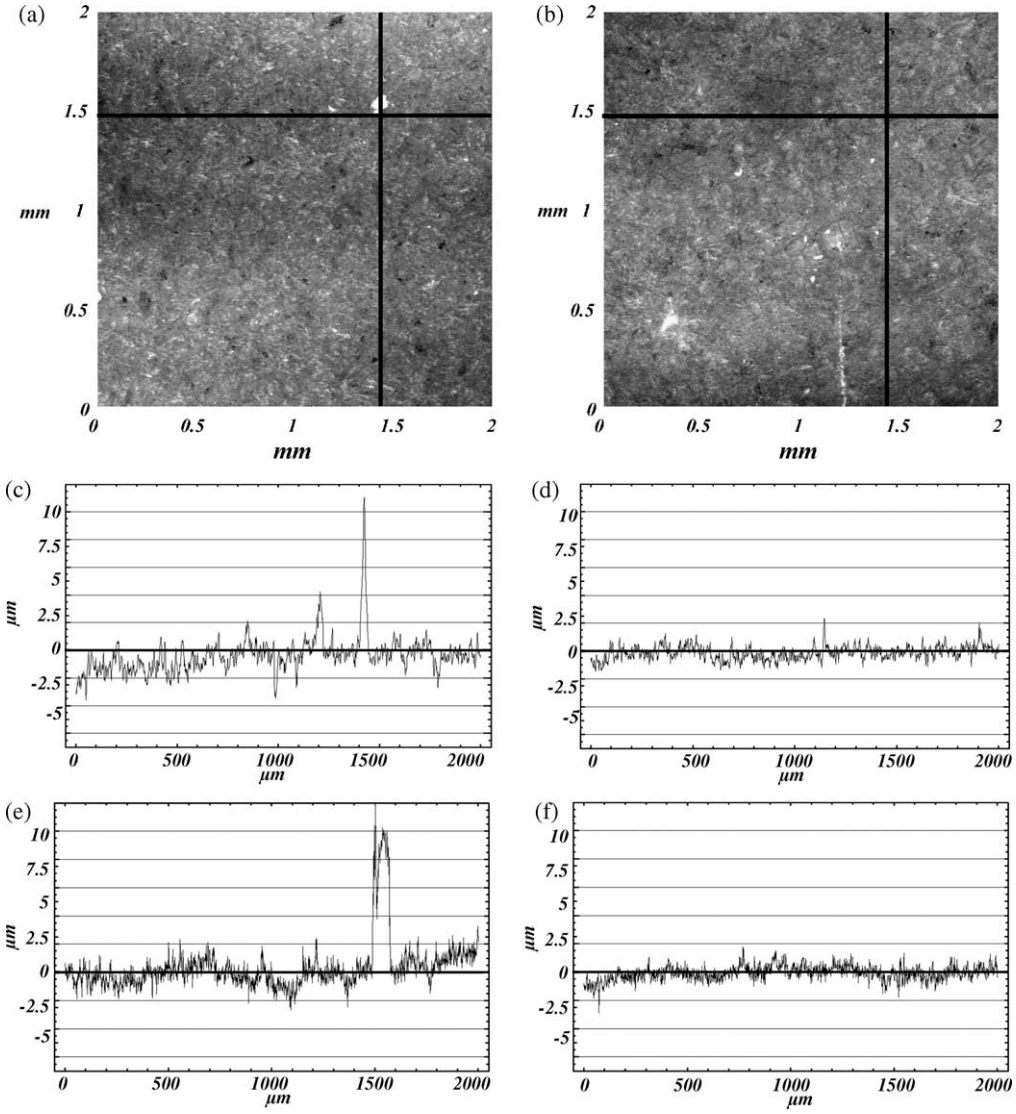

Fig. 4. Laser profilometer images of the theophylline anhydrate tablets (a) 30 kN theophylline anhydrate tablet, (b) 80 kN theophylline anhydrate tablet surface, (c) profile line (horizontal) from the Fig. 3a, (d) profile line (horizontal) from the Fig. 3b, (e) profile line (vertical) from the Fig. 3a and (f) profile line (vertical) from the Fig. 3b.

GMbH, Ettlingen, Germany) suggested that the higher compression pressure made the tablet surface smoother (Table 2). These values showed also that the roughness increased in order of KCl < NaCl < theophylline anhydrate < lactose monohydrate. In accordance with the matrix method the roughness values were calculated from the same 2 × 2 mm measurement areas which were divided in to 400 small squares from which the final roughness calculations were made. The obtained matrix method roughness values of showed that the 30 kN lactose monohydrate tablet was the roughest, which was also seen in Table 3. The higher compression pressure made the lactose monohydrate tablet clearly smoother which was also seen in the SEM images (Fig. 2a–d). With theophylline anhydrate tablets the compression pressure had smaller effect on the surface roughness. Variation of the roughness in different areas was higher with lactose monohydrate, theophylline anhydrate and also with the ionic salts when the lower compression pressure was used (Table 3). This suggests that there were larger degrees of heterogeneity on the surfaces when compression pressure was lower.

With KCl a larger variation in surface roughness was observed also with the higher compression pressure, which was due to a couple of rough spots on the surface. The higher compression pressure made the surface more homogeneous by filling the holes between surfaces with smaller fragmented particles. In an earlier study KCl and NaCl tablets were found to be relatively smooth, especially with the higher compression pressure [5]. The tablets made of KCl and NaCl showed that they were smoother than the lactose monohydrate tablets, but the difference in surface roughness between NaCl and theophylline anhydrate

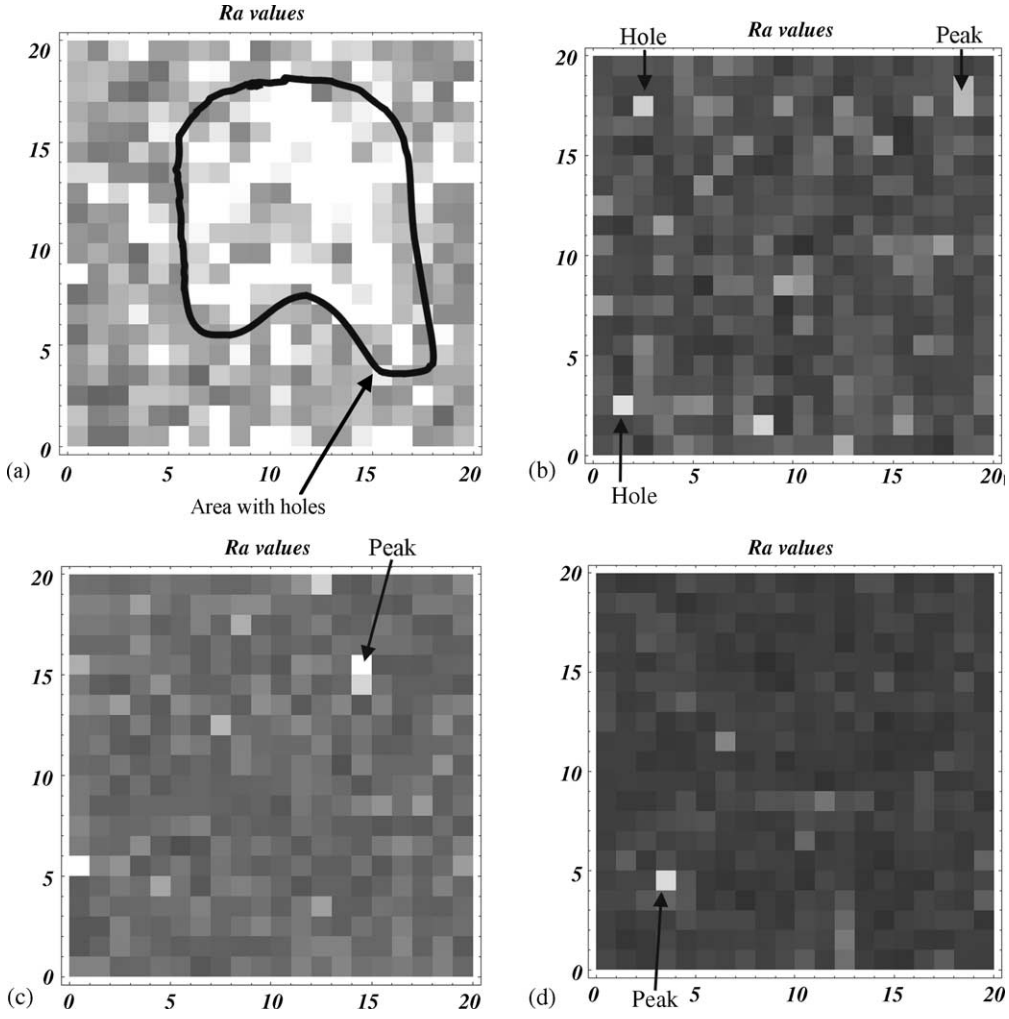

Fig. 5. Roughness value maps from the laser profilometer measurements of the tablets. The shade of the colour shows the scale of roughness (dark—small roughness, bright—large roughness). (a) 30 kN lactose monohydrate tablet (R_a range 0.48–2.60 μm, mean value 0.86 μm), (b) 80 kN lactose monohydrate tablet (R_a range 0.27–0.91 μm, mean value 0.42 μm), (c) 30 kN theophylline anhydrate tablet (R_a range 0.40–3.28 μm, mean value 0.53 μm) and (d) 80 kN theophylline anhydrate tablet (R_a range 0.26–0.89 μm, mean value 0.35 μm).

was small (Table 3). The comparison of the data given in Tables 2 and 3 seems to suggest that in one special case our new method will give higher roughness values for the 30 kN NaCl tablets than for the 30 kN theophylline anhydrate tablets. However, the standard deviation is especially high with 30 kN NaCl tablets and therefore such reasoning is not statistically significant. The high standard deviation is presumably due to the reflection problems of a laser beam

Table 2
R_a and R_{rms} roughness values of the tablet surfaces made by two compression forces (30 and 80 kN) and calculated using the standard method

Material (kN)	R_a	R_{rms}
Lactose monohydrate 30	0.96	1.39
Lactose monohydrate 80	0.56	0.77
Theophylline anhydrate 30	0.7	0.96
Theophylline anhydrate 80	0.42	0.55
KCl 30	0.4	0.6
KCl 80	0.24	0.4
NaCl 30	0.69	1.79
NaCl 80	0.38	0.5

Measurement area was 2×2 mm.

Table 3
R_a and R_{rms} roughness values of the tablet surfaces made by two compression forces (30 and 80 kN) and calculated using the matrix method

Material (kN)	R_a Mean ± SD (n = 400)	R_{rms} Mean ± SD (n = 400)
Lactose 30	0.86 ± 0.31	1.20 ± 0.40
Lactose 80	0.42 ± 0.09	0.58 ± 0.17
Theophylline 30	0.53 ± 0.17	0.70 ± 0.28
Theophylline 80	0.35 ± 0.05	0.45 ± 0.08
KCl 30	0.25 ± 0.12	0.36 ± 0.25
KCl 80	0.14 ± 0.14	0.21 ± 0.23
NaCl 30	0.61 ± 0.84	1.00 ± 1.33
NaCl 80	0.27 ± 0.07	0.36 ± 0.10

Measurement area was 2×2 mm which was divided in 400 small squares.

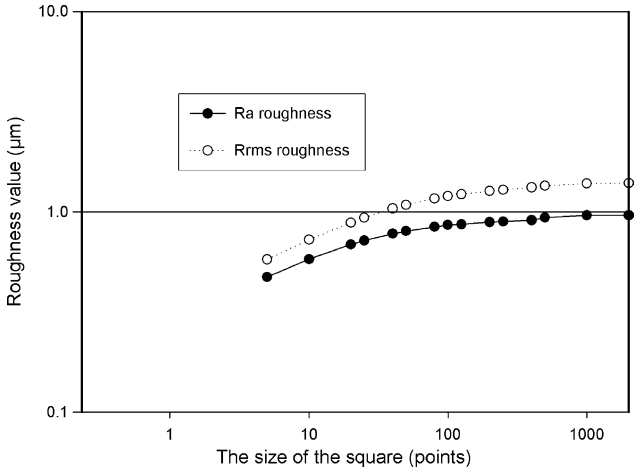

Fig. 6. Effect of the square size to the roughness values. The drawn lines show the common scaling behaviour which divides the curves into two regions by the size of the square.

from the NaCl tablet surface, since the largest holes may result in discontinuities in laser-beam reflection and cause small artefacts to the images.

Larger local roughness with lower compression pressure might be due to the elastic recovery of larger particles. In certain cases the lower compression pressure was not able to generate fragmentation or plastic flow of the particles. Therefore, the elastic behaviour was still significant also in the larger particles and this resulted a high local roughness values in some areas.

The roughness maps drawn from the roughness values of the matrix method agree with the laser profilometer images and the line profiles (Figs. 3a–d and 4a–f). When the original laser profilometer images show holes or high peaks, the roughness maps show large local roughness (marked in the Fig. 5a–d). These roughness maps also show surface heterogeneity, distribution of the roughness and the shade of the colour shows the scale of roughness (dark—small roughness, bright—large roughness). The roughness maps condense the amount of information given by the laser profilometer images which makes it easier to see the local roughness differences and the scale of roughness in the measurement area. This also helps the comparison of different measurements together. Dividing the measured area into small squares removes the effect of large scale height variations like uneven powder flow or uneven distribution of the powder in the tablet die. This visualisation technique makes it possible to notice roughness features which were caused by particle size and local compression pressure.

In our new matrix method it is also possible to calculate the roughness values for small squares so that the squares would, more or less, overlap each other. This overlapping of the squares increases the calculation time tremendously and therefore we have not used it in this study. The size of the measurement square which dictates the resolution influences significantly to the scale of the roughness values, like in all roughness measurements [13]. When the size of the square was changed gradually from 2000×2000 to 5×5 point, the fractal nature of the lactose monohydrate tablet surface was revealed (Fig. 6) [11,18]. In Fig. 6 the drawn lines show the common scaling behaviour which divides the curve into regions by the size of the square [11]. Furthermore, it is possible to extend the matrix method easily for other roughness parameters or fractal dimensions and get visual images of the local variations of these parameters. The method described is not limited to the presented measurement technique or to the scale used in this study. The method described can be used with any roughness measurement which produces numeral data e.g. atomic force microscopy.

4. Conclusions

The proposed new method to visualise surface roughness gives easily detailed roughness maps. These maps are able to show local variations in surface roughness values and provide a picture of the surface heterogeneity. Although, the test material is still quite limited the results suggested that the new method is promising in characterisation of tablet surfaces. It seems also quite evident that the same calculations can be easily extended for other roughness parameters or fractal dimensions and get visual images of the local variations of these parameters. The results also showed that higher compression pressure resulted to smoother tablet surfaces, because the boundary lines between larger powder particles were filled with smaller fragmented particles.

Acknowledgements

This study was financially supported by The National Technology Agency of Finland (TEKES). Niklas Laitinen is acknowledged for his help in the image analysis of the powders.

References

[1] F. Podczeck, Measurement of surface roughness of tablets made from polyethylene glycol powders of various molecular weight, Pharm. Pharmacol. Commun. 4 (1998) 179–182.
[2] M. Riippi, O. Antikainen, T. Niskanen, J. Yliruusi, The effect of compression force on surface structure, crushing strength, friability, and disintegration time of erythromycin acistrate tablets, Eur. J. Pharm. Biopharm. 46 (1998) 339–345.
[3] M. Salako, F. Podczeck, M. Newton, Investigations into the deformability and tensile strength of pellets, Int. J. Pharm. 168 (1998) 49–57.
[4] M. Ruotsalainen, J. Heinämäki, O. Antikainen, J. Yliruusi, Time-dependent dimensional cahnges and film adhesion of coated tablets, S.T.P.Pharma Sci. 12 (2002) 385–389.

[5] P. Seitavuopio, J. Rantanen, J. Yliruusi, Tablet surface characterisation by various imaging techniques, Int. J. Pharm. 254 (2003) 281–286.
[6] P. Wagberg, P.-A. Johansson, Surface profilometry—a comparison between optical and mechanical sensing on printing papers, Tappi J. 46 (1993) 115–121.
[7] Y.-J. Cho, Y.P. Koo, J.-H. Jeon, Surface profile estimation by digital filtering for wear volume calculation, Wear 252 (2002) 173–178.
[8] P.F. Chauvy, C. Madore, D. Landolt, Variable length scale analysis of surface topography: characterisation of titanium surfaces for biomedical applications, Surf. Coat. Technol. 110 (1998) 48–56.
[9] P.A. Burrough, Fractals and geochemistry, in: D. Avnir (Ed.), The Fractal Approach to Heterogeneous Chemistry (Surfaces, Colloids, Polymers), Wiley, New York, NY, USA, 1989, pp. 383–406.
[10] A. Malinverno, A simple method to estimate the fractal dimension of self-affine series, Geophys. Res. Lett. 17 (1990) 1953–1956.
[11] T. Yoshinobu, A. Iwamoto, H. Iwasaki, Mesoscopic roughness characterization of grown surfaces by atomic force microscopy, Jpn J. Appl. Phys. 33 (Part 2) (1994) L67–L69.
[12] T. Li, K. Park, Fractal analysis of pharmaceutical particles by atomic force microscopy, Pharm. Res. 15 (1998) 1222–1232.
[13] H. Zahouani, R. Vargiolu, Ph. Kapsa, J.L. Loubet, T.G. Mathia, Effect of lateral resolution on topographical images and three-dimensional function parameters, Wear 219 (1998) 114–123.
[14] R.J. Roberts, R.C. Rowe, The effect of the relationship between punch velocity and particle size on the compaction behaviour of materials with varying deformation mechanisms, J. Pharm. Pharmacol. 38 (1986) 567–571.
[15] G.K. Bolhuis, Z.T. Chowhan, Materials for direct compaction, in: G. Alderborn, C. Nyström (Eds.), Pharmaceutical Powder Compaction Technology, Marcel Dekker, New York, NY, USA, 1996, pp. 461–500.
[16] P. Narayan, B.C. Hancock, The relationship between the particle properties, mechanical behavior, and surface roughness of some pharmaceutical excipient compacts, Mater. Sci. Eng. A 355 (2003) 24–36.
[17] E. Suihko, V.-P. Lehto, J. Ketolainen, E. Laine, P. Paronen, Dynamic solid-state and tableting properties of four theophylline forms, Int. J. Pharm. 217 (2001) 225–236.
[18] S.J. Fang, S. Haplepete, W. Chen, C.R. Helms, H. Edwards, Analyzing atomic force microscopy images using spectral methods, J. Appl. Phys. 82 (1997) 5891–5895.